Inorganic Chemistry

pubs.acs.org/IC
Article

Polycationic Ru(II) Luminophores: Syntheses, Photophysics, and Application in Electrostatically Driven Sensitization of Lanthanide Luminescence

Richard C. Knighton,* Joseph M. Beames, and Simon J. A. Pope*

Cite This: *Inorg. Chem.* 2023, 62, 19446−19456
Read Online

ABSTRACT: A series of photoluminescent Ru(II) polypyridine complexes have been synthesized in a manner that varies the extent of the cationic charge. Two ligand systems (L1 and L2), based upon 2,2′-bipyridine (bipy) mono- or difunctionalized at the 5- or 5,5′-positions using *N*-methylimidazolium groups, were utilized. The resulting Ru(II) species therefore carried +3, +4, +6, and +8 complex moieties based on a $[Ru(bipy)_3]^{2+}$ core. Tetra-cationic $[Ru(bipy)_2(\mathbf{L2})][PF_6]_4$ was characterized using XRD, revealing H-bonding interactions between two of the counteranions and the cationic unit. The ground-state features of the complexes were found to closely resemble those of the parent unfunctionalized $[Ru(bipy)_3]^{2+}$ complex. In contrast, the excited state properties produce a variation in emission maxima, including a bathochromic 44 nm shift of the ^{3}MLCT band for the tetra-cationic complex; interestingly, further increases in overall charge to +6 and +8 produced a hypsochromic shift in the ^{3}MLCT band. Supporting DFT calculations suggest that the trend in emission behavior may, in part, be due to the precise nature of the LUMO and its localization. The utility of a photoactive polycationic Ru(II) complex was then demonstrated through the sensitization of a polyanionic Yb(III) complex in free solution. The study shows that electrostatically driven ion pairing is sufficient to facilitate energy transfer between the ^{3}MLCT donor state of the Ru(II) complex and the accepting $^2F_{5/2}$ excited state of Yb(III).

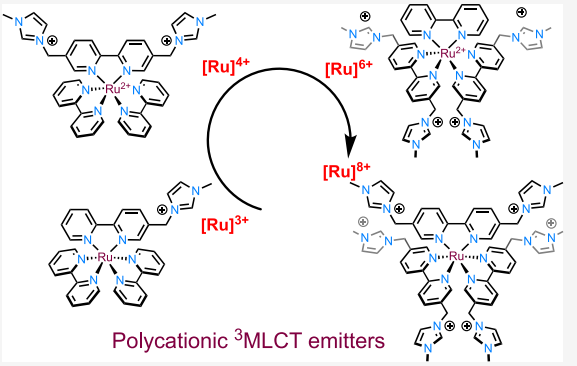

INTRODUCTION

The study of photoactive transition-metal complexes is a rich and diverse area of chemistry and has important applications in many areas, such as light harvesting,[1−3] sensing,[4,5] energy upconversion,[6−8] bioimaging,[4] and theranostics.[10,11,11] While interest in earth-abundant luminescent complexes[13] has understandably, from a sustainability perspective, attracted significant attention in the past few years, precious metals still provide an excellent basis for the rational design of efficient photoluminescent compounds.

Our interest has been drawn to the study of (poly)cationic luminescent complexes and their potential applications. In particular, cationic complexes are important in host−guest studies;[14] as components of ionic liquids;[15] ion pairing;[16] in the development of sensors and DNA binding;[17] as photoactive components of aggregation colloids such as micelles and microemulsions;[18] and, in membrane transport studies.[19] However, luminescent metal complexes with high magnitudes of overall positive charge are very rare. Therefore, we were interested in investigating the synthesis and physical properties of a series of cationic Ru(II) complexes that are structurally related to the archetypal triplet metal to ligand charge transfer (^{3}MLCT) emitter $[Ru(bipy)_3]^{2+}$ (where bipy = 2,2′-bipyridine).

Recently, the early history of bipy has been retrospectively reviewed by Constable and Housecroft[20] providing an important reminder of the ubiquity and ongoing application of this ligand and its close relatives. Ligand modification is the obvious route for the consideration of polycationic luminescent Ru(II) complexes, and our approach, described herein, was facilitated by the use of cationic bipy ligands. Interestingly, anionic bipy ligands are more common in the literature, for example carboxylated (some of the earliest reported variants of bipy[21]) or phosphonated[22] derivatives of bipy are very well known and have been widely exploited in coordination chemistry.[23] Although rarer, cationic bipyridines have been reported and complexed with Ru(II). Typically, these ligands incorporate terminal amine groups that can be protonated in certain media, allowing their development as luminescent sensors, or for consideration in photodynamic therapy, which exploits the inherent phototoxicity of the Ru(II) complex.[24]

Received: July 11, 2023
Revised: November 2, 2023
Accepted: November 3, 2023
Published: November 20, 2023

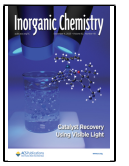

https://doi.org/10.1021/acs.inorgchem.3c02352
Inorg. Chem. 2023, 62, 19446−19456

Meyer and co-workers reported a series of Ru(II) complexes with quaternary alkylated amine substituents at the 4,4′ positions of the bipy framework; the complexes were studied in the context of Ru-based dye-sensitized solar cells where the effect of charge and ion pairing with iodide is especially important.[25] Similar cationic ligands have been deployed in heteroleptic Ru(II) complexes that show a very high affinity for DNA (via intercalation) and subsequent in vitro activity in antitumor experiments.[26]

An additional aim of the current work on polycationic Ru(II) complexes was to investigate whether such species could be used as sensitizers of trivalent lanthanide excited states. In that context, it is now two decades since transition metal complexes were first demonstrated[27] to be viable chromophores for sensitized lanthanide luminescence. In particular, MLCT species such as derivatives of the aforementioned $[Ru(bipy)_3]^{2+}$ can sensitize lanthanide ions (for example, Nd(III), Yb(III), and Er(III), all of which are near-IR emitters) which possess accepting excited states that are compatible with the donor ^{3}MLCT energy level. Typically the lanthanide excited state is populated through energy transfer mechanisms.[28] Generally, these mixed-metal, so-called d-f hybrids,[29] have been obtained through covalently linked ditopic ligands,[30] or self-assembly of complex components,[31] including through supramolecular host−guest interactions.[32] This current work demonstrates that favorable electrostatic interactions in solution can be manipulated to promote energy transfer between polycationic Ru(II) and anionic Yb(III) complexes.

EXPERIMENTAL SECTION

^{1}H and ^{13}C{^{1}H} NMR spectra were recorded on an NMR-FT Bruker 500 MHz spectrometer and recorded in $CDCl_3$, acetonitrile-d_3, and DMSO-d_6. ^{1}H and ^{13}C{^{1}H} NMR chemical shifts (δ) were determined relative to residual solvent peaks with digital locking and are given in ppm. Coupling constants are quoted in Hz. High-resolution mass spectra were obtained at Cardiff University. UV−vis studies were performed on a Shimadzu UV-1800 spectrophotometer as MeCN solutions (1×10^{-5} M). Photophysical data were obtained on a JobinYvon−Horiba Fluorolog spectrometer fitted with a JY TBX picosecond photodetection module. A Hamamatsu R5509−73 detector (cooled to −80 °C using a C9940 housing) was used for near-IR measurements. Luminescence lifetime profiles were obtained using the JobinYvon−Horiba FluoroHub single photon counting module, and the data fits yielded the lifetime values using the provided DAS6 deconvolution software. The pulsed source was a nano-LED configured for 295 nm output operating at 1 MHz; for the near-IR Yb(III) lifetimes, the pulsed laser source was a Continuum Minilite Nd:YAG configured for 355 nm output. Quantum yield measurements were obtained using comparative actinometry on aerated MeCN solutions of the complexes using $[Ru(bipy)_3](PF_6)_2$ in aerated MeCN as a standard ($\Phi = 0.018$).[33] Elemental analyses were conducted by the EA Services Team at the London Metropolitan University.

CYCLIC VOLTAMMETRY

Cyclic voltammetry was performed by using a PalmSens4 potentiostat. Experiments were performed using HPLC grade CH_2Cl_2 with an analyte concentration of 1 mM at 293 K, using triply recrystallized $[^nBu_4N][PF_6]$ as the supporting electrolyte at 0.1 M concentration. A three-electrode setup was used, consisting of a platinum disc working electrode, a platinum wire counter-electrode, and a silver wire pseudoreference. Solutions were sparged for 10 min with a CH_2Cl_2 saturated stream of nitrogen gas. Voltammograms were referenced to the ferrocene/ferrocenium redox couple measured by using the same conditions.

COMPUTATIONAL METHODS

Electronic structure calculations were performed using density functional theory within the Gaussian 09 computational chemistry suite.[34] All calculations were performed with the Stuttgart−Dresden (SDD) effective core potential and basis set in the treatment of the ruthenium,[35] in combination with a 6-31G* basis set for all other light atoms.[36] Geometry optimizations were performed for all cationic species, and minima were confirmed as stationary points through the computation of harmonic vibrational frequencies, each of which showed no imaginary components. These stationary points were used in single-point TD-DFT calculations to compute vertical excitation energies. Calculations were performed on isolated complexes without implicit solvent due to substantial difficulties in converging both SCF and geometry optimization components of the higher charge complexes through the SCRF formalization.

Phosphorescence and spin-forbidden absorption band positions are estimated using triplet-inclusive TD-DFT calculations. Decomposition of the molecular orbital character was performed using the GaussSum software package.[37]

X-RAY CRYSTALLOGRAPHY

Data Collection and Processing. A suitable crystal was selected and mounted on a nylon loop with Fomblin oil and placed on a Rigaku Oxford Diffraction SuperNova diffractometer with a dual source (Cu at zero) equipped with an AtlasS2 CCD area detector at 293(2) K. The crystal was kept at a steady T of 293(2) K during data collection. The structure was solved with the SHELXT[38] structure solution program using the Intrinsic Phasing solution method and by using Olex2[39] as the graphical interface. The model was refined with SHELXL[40] using the least-squares minimization. CCDC 2250505 contains the supplementary X-ray crystallographic data for $[Ru(bipy)_2(\mathbf{L2})][PF_6]_4$. These data can be obtained free of charge from the Cambridge Crystallographic Data Centre via www.ccdc.cam.ac.uk/data_request/cif., or from the Cambridge Crystallographic Data Centre, Union Road, Cambridge, CB2 1EZ; fax(+44) 1223−336−033 or email: deposit@ccdc.cam.ac.uk.

Synthesis of the Ligands. *Synthesis of 3-([2,2′-Bipyridin]-5-ylmethyl)-1-methyl-1H-imidazol-3-ium Chloride (**L1**).* 5-chloromethyl-2,2′-bipyridine (800 mg, 3.91 mmol, 1.0 equiv) was dissolved in 1-methylimidazole (24 mL) and heated under N_2 at 100 °C for 3 h. The reaction was cooled to ambient temperature, and Et_2O (72 mL) was added. The mixture was cooled to 4 °C for 18 h, filtered, washed with Et_2O (2 × 10 mL), and dried in vacuo to obtain the compound as a hygroscopic deliquescent off-white solid (0.870 g, 3.03 mmol, 78%). ^{1}H NMR spectrum (500 MHz, 293 K, CD_3OD): 9.17 (s, 1H, ImH, 97% deuterated in CD_3OD), 8.78 (s, 1H, bipyH), 8.66 (d, $^3J_{HH}$ = 4.7, 1H, bipyH), 8.38 (d, $^3J_{HH}$ = 8.4, 1H, bipyH), 8.36 (d, $^3J_{HH}$ = 8.0, 1H, bipyH), 8.02 (d, $^3J_{HH}$ = 8.2, $^4J_{HH}$ = 2.2, 1H, bipyH), 7.94 (app. t, J_{HH} = 7.7, 1H, bipyH), 7.75 (s, 1H, ImH), 7.65 (s, 1H, ImH), 7.47−7.34 (m, 1H, bipyH), 5.60 (s, 2H, $ArCH_2$), 3.97 (s, 3H, NCH_3); ^{13}C{^{1}H} NMR spectrum (126 MHz, 293 K, CD_3OD): 157.9 (s, bipy), 156.5 (s, bipy), 156.4 (s, bipy), 150.4 (s, bipy), 138.8 (s, bipy), 138.7 (s, bipy), 138.1 (t, $^1J_{CD}$ = 34, Im deuterated), 131.6 (s, bipy), 125.7 (s, bipy), 125.5 (s, Im), 123.7 (s, Im), 122.7 (s, bipy), 122.6 (s, bipy), 51.2 (s, $ArCH_2$), 36.7 (s, NCH_3), only the deuterated imidazolium resonance observed. Elemental analysis: found: C 60.75%, H 5.24%, N 18.47%; calcd for

https://doi.org/10.1021/acs.inorgchem.3c02352
Inorg. Chem. 2023, 62, 19446−19456

$C_{15}H_{15}N_4Cl_{0.5}H_2O$, C 60.91%, H 5.45%, N 18.94%. ESI-MS m/z calcd for $[C_{15}H_{15}N_4]^+$, 251.1297; found, 251.1301. IR (ATR): ν_{max} 3382, 3069, 2943, 2859, 1574, 1460, 1177, 1024, 847 cm^{-1}.

*Synthesis of 3,3′-([2,2′-Bipyridine]-5,5′-diylbis-(methylene))bis(1-methyl-1H-imidazol-3-ium) Dichloride (**L2**).* 5,5′-bischloromethyl-2,2′-bipyridine (870 mg, 3.44 mmol, 1.0 equiv) was dissolved in 1-methylimidazole (30 mL) and heated to 100 °C for 18 h. The reaction was cooled to ambient temperature and Et_2O (90 mL) was added. The reaction was stirred for 10 min, filtered, and the solid was washed with Et_2O (2 × 60 mL) to obtain the product as a hygroscopic off-white solid (1.43 g, 0.34 mmol, >99%). ^1H NMR spectrum (500 MHz, 293 K, CD_3OD): 9.14−9.11 (m, 2H, ImH, 25% deuterated), 8.80−8.75 (m, 2H, bipyH), 8.46 (dd, $^3J_{HH}$ = 8.2, $^4J_{HH}$ = 0.8, 2H, bipyH), 8.04−7.99 (m, 2H, bipyH), 7.73 (app.t, J_{HH} = 1.9, 2H, ImH), 7.64 (app.t, J_{HH} = 1.9, 2H, ImH), 5.58 (s, 4H, $ArCH_2$), 3.96 (s, 6H, NCH_3); $^{13}C\{^1H\}$ NMR spectrum (126 MHz, 293 K, CD_3OD): 156.9 (s, bipy), 150.6 (s, bipy), 139.0 (s, bipy), 138.7−137.9 (m, Im-deuterated), 137.5 (s, Im−nondeuterated), 132.1 (s, bipy), 125.5 (s, Im), 123.6 (s, Im), 122.6 (s, bipy), 51.1(s, $ArCH_2$), 36.8 (NCH_3) ppm. ESI-MS m/z calcd for $[C_{20}H_{22}N_6]^+$, 381.1595; found, 381.1590. IR (ATR): ν_{max} 3354, 3055, 2945, 2858, 1576, 1557, 1454, 1174, 1024, 785 cm^{-1}.

Synthesis of the Complexes. *Synthesis of [Ru-(bipy)$_2$(**L1**)][PF$_6$]$_3$.* A Schlenk flask was charged with 3,3′-([2,2′-bipyridine]-5,5′-diylbis(methylene))bis(1-methyl-1*H*-imidazol-3-ium) dichloride (103.5 mg, 0.248 mmol, 1.05 equiv) and $[Ru(bipy)_2Cl_2]$ (114.4 mg, 0.236 mmol, 1.0 equiv) under N_2. Ethylene glycol (2 mL) was added, and the solvent was sparged with N_2 for 15 min. The reaction was heated to reflux for 3 h after which the reaction was cooled and $NH_4PF_{6(aq)}$ (0.1 M, 10 mL) was added. The solid was filtered, and the crude material was purified by column chromatography (SiO_2; MeCN/H_2O/sat. $KNO_{3(aq)}$; 20:2:1 → 14:2:1). The organic solvent was removed, and the product precipitated via the addition of $NH_4PF_{6(aq)}$ (0.1 M, 10 mL). The solid was filtered and washed with H_2O (2 × 2 mL) and dried to give the title compound as a red solid (132 mg, 0.098 mmol, 60%). ^1H NMR spectrum (500 MHz, 293 K, CD_3CN): 8.55−8.47 (m, 6H, bipyH), 8.43−8.40 (m, 1H, ImH), 8.11−8.02 (m, 6H, bipyH), 7.92 (dd, $^3J_{HH}$ = 8.4, $^4J_{HH}$ = 2.1, 1H, bipyH), 7.78 (ddt, $^3J_{HH}$ = 5.5, $^4J_{HH}$ = 1.5, 0.7, 1H, bipyH), 7.76−7.67 (m, 4H, bipyH), 7.52 (m, 1H, bipyH), 7.45−7.38 (m, 5H, bipyH), 5.29 (d, $^2J_{HH}$ = 16.0, 1H, $ArCH_2$), 5.24 (d, $^2J_{HH}$ = 16.0, 1H, $ArCH_2$), 3.83 (s, 3H, $ImCH_3$); $^{13}C\{^1H\}$ NMR spectrum (126 MHz, 293 K, CD_3CN): 158.3 (s, bipy), 158.0 (s, bipy), 158.0 (s, bipy), 157.4 (s, bipy), 153.0 (s, bipy), 153.0 (s, bipy), 152.9 (s, bipy), 152.8 (s, bipy), 152.7 (s, bipy), 152.6 (s, bipy), 151.4 (s, bipy), 138.9 (s, bipy), 138.9 (s, bipy), 138.9 (s, bipy), 138.8 (s, bipy), 138.0 (s, bipy),137.9 (s, Im), 135.1 (s, bipy), 128.9 (s, bipy), 128.6 (s, bipy), 128.6 (s, bipy), 125.8 (s, Im), 125.4 (s, bipy), 125.4 (s, Im), 125.3 (s, bipy), 125.3 (s, bipy), 125.2 (s, bipy), 123.5 (s, bipy), 118.4 (s, bipy), 50.2 (s, $ArCH_2$), 37.1 (s, $ImCH_3$) ppm. ESI-MS m/z calcd for $[C_{35}H_{31}F_{12}N_8P_2Ru]^+$, 955.1008; found, 955.1010. IR (ATR): ν_{max} 1466, 1445, 758, 729, 648, 623, 556, 419 cm^{-1}.

*Synthesis of [Ru(bipy)$_2$(**L2**)][PF$_6$]$_4$.* A Schlenk flask was charged with 3-([2,2′-bipyridin]-5-ylmethyl)-1-methyl-1*H*-imidazol-3-ium chloride (34.7 mg, 0.121 mmol, 1.05 equiv) and $[Ru(bipy)_2Cl_2]$ (55.8 mg, 0.115 mmol, 1.0 equiv) under N_2. Ethylene glycol (1 mL) was added, and the solvent was sparged with N_2 for 15 min. The reaction was heated to reflux for 3 h after which the reaction was cooled and $NH_4PF_{6(aq)}$ (0.1 M, 10 mL) was added. The solid was filtered, and the crude material was purified by column chromatography (SiO_2; MeCN/H_2O/sat. $KNO_{3(aq)}$; 14:2:1). The organic solvent was removed in vacuo and the product precipitated via the addition of $NH_4PF_{6(aq)}$ (0.1 M, 10 mL). The solid was filtered and washed with H_2O (2 × 2 mL) and dried to give the title compound as a red solid (76 mg, 0.069 mmol, 42%). ^1H NMR spectrum (500 MHz, 293 K, CD_3CN): 8.55−8.45 (m, 6H, bipyH), 8.38 (s, 2H, ImH), 8.11−8.05 (m, 4H, bipyH), 7.91 (dd, $^3J_{HH}$ = 8.5, $^4J_{HH}$ = 2.0, 2H, bipyH), 7.72 (ddd, $^3J_{HH}$ = 5.6, $^4J_{HH}$ = 1.5, 0.7, 2H, bipyH), 7.65 (ddd, $^3J_{HH}$ = 5.6, $^4J_{HH}$ = 1.5, 0.7, 2H), 7.53−7.48 (m, 2H, bipyH), 7.43 (ddd, $^3J_{HH}$ = 7.7, 5.6, $^4J_{HH}$ = 1.3, 2H), 7.39 (ddd, $^3J_{HH}$ = 7.7, 5.6, $^4J_{HH}$ = 1.3, 2H), 7.34 (app.t, J_{app} = 1.8, 2H, ImH), 7.20 (app.t, J_{app} = 1.9, 2H, ImH), 5.27 (d, $^2J_{HH}$ = 16.3, 2H, ArCHH), 5.23 (d, $^2J_{HH}$ = 16.3, 2H, ArCHH), 3.82 (s, 6H, $ImCH_3$); $^{13}C\{^1H\}$ NMR spectrum (126 MHz, 293 K, CD_3CN), 157.9 (s, bipy), 157.9 (s, bipy), 157.7 (s, bipy), 152.9 (s, bipy), 152.7 (s, bipy), 151.5 (s, bipy), 139.0 (s, bipy), 138.9 (s, bipy), 138.0 (s, bipy), 137.9 (s, Im), 135.4 (s, bipy), 128.7 (s, bipy), 128.6 (s, bipy), 125.6 (s, bipy), 125.4 (s, Im), 125.3 (s, bipy), 123.5 (s, Im), 50.2 (s, $ArCH_2$), 37.1 (s, $ImCH_3$) ppm. ESI-MS m/z calcd for $[C_{40}H_{38}N_{10}Ru]^+$, 190.0584; found, 190.0583. IR (ATR): ν_{max} 1466, 1446, 1167, 759, 642, 623, 556, 470, 419 cm^{-1}.

*Synthesis of [Ru(**L2**)$_2$Cl$_2$]Cl$_4$.* A Schlenk flask was charged with $[Ru(DMSO)_4Cl_2]$ (69.7 mg, 0.144 mmol, 1.0 equiv), LiCl (48.8 mg, 1.15 mmol, 8.0 equiv), and 3-([2,2′-bipyridin]-5-ylmethyl)-1-methyl-1*H*-imidazol-3-ium chloride (120 mg, 0.288 mmol, 2.0 equiv) under N_2. EtOH (10 mL) was added, and the solution was sparged with N_2 for 15 min. The reaction was heated to reflux for 18 h, after which it was cooled and the solvent was removed in vacuo. The crude material was purified by column chromatography (Al_2O_3; acetone/H_2O; 100:0 → 50:50) and the solvent was removed in vacuo to give the title compound as a purple solid (20 mg, 0.020 mmol, 14%). ^1H NMR spectrum (300 MHz, 293 K, CD_3OD) 9.89 (d, $^4J_{HH}$ = 2.0, 2H, bipyH), 8.66 (d, $^3J_{HH}$ = 8.6, 2H, bipyH), 8.50 (d, $^3J_{HH}$ = 8.4, 2H, bipyH), 8.13 (dd, $^3J_{HH}$ = 8.4, $^4J_{HH}$ = 2.1, 1H, bipyH), 7.91 (d, $^3J_{HH}$ = 2.0, 2H, ImH), 7.85 (d, $^3J_{HH}$ = 1.8, 2H, ImdH), 7.73 (dd, $^3J_{HH}$ = 8.5, $^4J_{HH}$ = 2.0, 2H, bipyH), 7.69 (d, $^3J_{HH}$ = 2.0, 2H, ImH), 7.61 (d, $^3J_{HH}$ = 2.0, 2H, ImH), 7.56 (d, $^3J_{HH}$ = 2.0, 2H. ImH), 5.85 (d, $^2J_{HH}$ = 15.4, 2H, $ArCH_2$), 5.76 (d, $^2J_{HH}$ = 15.4, 2H, $ArCH_2$), 5.39 (s, 4H, $ArCH_2$), 3.99 (s, 6H, $ImCH_3$), 3.92 (s, 6H, $ImCH_3$). The remaining imidazolium N−CH−N protons were undetected due to deuteration. $^{13}C\{^1H\}$ NMR spectrum (126 MHz, 293 K, CD_3OD): 161.8 (s, bipy), 159.9 (s, bipy), 154.0 (s, bipy), 153.7 (s, bipy), 139.0−137.9 (m, ImCD, deuterated), 136.7 (s, bipy), 135.6 (s, bipy), 125.5 (s, Im), 125.4 (s, Im), 124.9 (s, bipy), 124.7 (s, bipy), 124.2 (s, Im), 123.8 (s, Im), 51.2 (s, $ArCH_2$), 50.2 (s, $ArCH_2$), 36.9 (s, $ImCH_3$), 36.8 (s, $ImCH_3$) ppm. ESI-MS m/z calcd for $[C_{40}H_{44}Cl_2N_{12}Ru]^{4+}$, 216.0559; found, 216.0572.

*Synthesis of [Ru(bipy)(**L2**)$_2$][PF$_6$]$_6$.* A Schlenk flask was charged with [Ru(bipy)(*p*-cymene)Cl]Cl (54.5 mg, 0.114 mmol, 1.0 equiv) and 3-([2,2′-bipyridin]-5-ylmethyl)-1-methyl-1*H*-imidazol-3-ium chloride (100 mg, 0.239 mmol, 2.1 equiv) under N_2. 2-Ethoxyethanol (1 mL) was added, and the reaction was sparged with N_2 for 15 min. The reaction was heated to reflux for 48 h after which the reaction was cooled and the compound precipitated via the addition of $NH_4PF_{6(aq)}$

https://doi.org/10.1021/acs.inorgchem.3c02352
Inorg. Chem. 2023, 62, 19446−19456

Scheme 1. Synthetic Routes to the Family of Homologous Polycationic ruthenium(II) Bipyridine Complexes

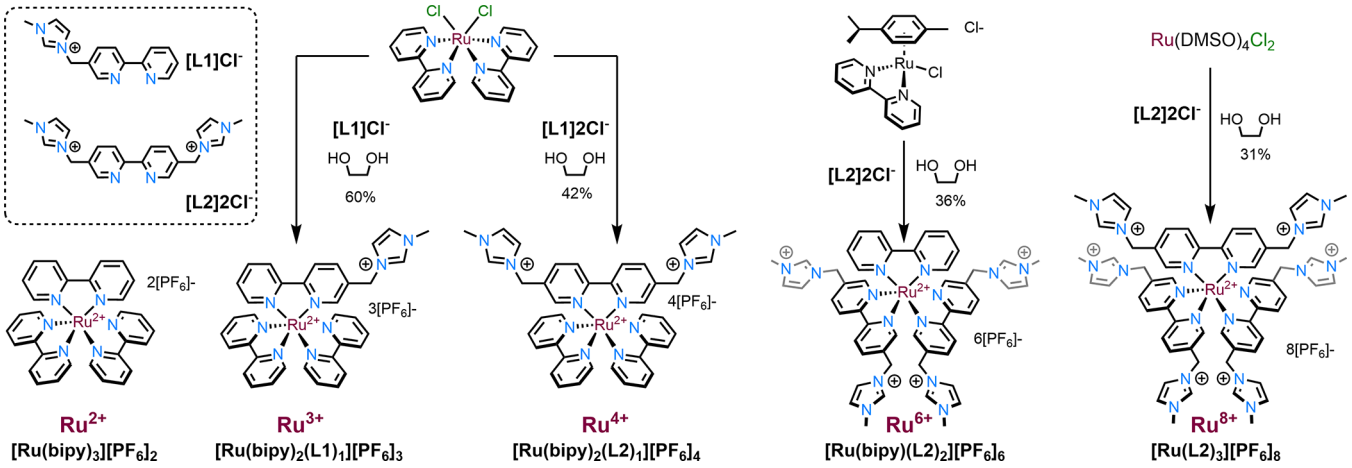

(0.1 M, 10 mL). The solid was filtered and washed with H_2O (2 × 5 mL). The crude mixture was purified by column chromatography (SiO_2; MeCN/H_2O/sat. $KNO_{3(aq)}$; 14:2:1 → 9:10:1). The organic solvent was removed in vacuo and the compound precipitated via the addition of $NH_4PF_{6(aq)}$ (0.1 M, 10 mL). The solid was filtered and washed with H_2O (2 × 5 mL) and dried in vacuo to give the title compound as a red solid (75 mg, 0.041 mmol, 36%). ^{1}H NMR spectrum (500 MHz, 293 K, CD_3CN) 8.54−8.49 (m, 4H, bipyH), 8.46 (dt, $^3J_{HH}$ = 8.1, $^4J_{HH}$ = 1.1, 2H), 8.44−8.40 (m, 2H, ImH), 8.37 (m, 2H, ImH), 8.10 (app.td, J_{app} = 7.9, $^4J_{HH}$ = 1.5, 2H, bipyH), 7.89 (dd, $^3J_{HH}$ = 8.6, $^4J_{HH}$ = 1.9, 2H, bipyH), 7.85 (dd, $^3J_{HH}$ = 8.5, $^4J_{HH}$ = 2.0, 2H, bipyH), 7.69−7.66 (m, 2H, bipyH), 7.64−7.61 (m, 2H, bipyH), 7.52−7.50 (m, 2H, bipyH), 7.43−7.40 (m, 2H, bipyH), 7.39 (app.t, J_{app} = 1.7, 2H, ImH), 7.36 (app.t, J_{app} = 1.7, 2H, ImH), 5.26 (d, $^2J_{HH}$ = 16.1, 2H, ArCHH), 5.25 (s, 4H, $ArCdH_2$), 5.23 (d, $^2J_{HH}$ = 16.2, 2H, ArCHH), 3.85 (s, 6H, $ImCH_2$), 3.83 (s, 6H, $ImCH_2$); $^{13}C\{^1H\}$ NMR spectrum (126 MHz, 293 K, CD_3CN) 157.6 (s, bipy), 157.6 (s, bipy), 157.5 (s, bipy), 153.0 (s, bipy), 151.9 (s, bipy), 151.5 (s, bipy), 139.0 (s, bipy), 138.1 (s, bipy), 137.9 (s, bipy), 137.8 (s, Im), 135.3 (s, bipy), 135.2 (s, bipy), 128.7 (s, bipy), 125.7 (s, bipy), 125.5 (s, bipy), 125.3 (s, Im), 125.3 (s, Im), 125.2 (s, bipy), 123.4 (s, Im), 123.3 (s, Im), 50.1 (s, bipy), 50.0 (s, $ArCH_2$), 50.0 (s, $ArCH_2$), 36.7 (s, $ImCH_3$) ppm. ESI-MS *m/z* calcd for $[C_{50}H_{52}F_{24}N_{14}P_4Ru]^{2+}$, 765.1061; found, 765.1061. IR (ATR): ν_{max} 3169, 3125, 2349, 2326, 1604, 1577, 1566, 1467, 446, 1425, 1400, 1160, 760, 741, 731, 669, 648, 623, 516 cm^{-1}.

*Synthesis of [Ru(**L2**)$_3$][PF$_6$]$_8$.* A Schlenk flask was charged with $[Ru(DMSO)_4Cl_2]$ (38.7 mg, 0.080 mmol, 1.0 equiv) and 3-([2,2′-bipyridin]-5-ylmethyl)-1-methyl-1*H*-imidazol-3-ium chloride (100 mg, 0.240 mmol, 3.0 equiv) under N_2. Ethylene glycol (2 mL) was added, and the reaction was sparged with N_2 for 15 min. The reaction was refluxed for 3 h after which the reaction was cooled and the product precipitated as an oil via dropwise addition to stirring THF (100 mL). The solution was decanted and the product coevaporated with MeOH (2 × 5 mL). The compound was purified by column chromatography (Al_2O_3; acetone/H_2O; 100:0 → 50:50). The solvent was removed in vacuo and the oil redissolved in H_2O (3 mL) and precipitated via the addition of $NH_4PF_{6(aq)}$ (0.1 M, 3 mL). The solid was filtered and dried in vacuo to give the title compound as an orange solid (54 mg, 0.023 mmol, 31%). ^{1}H NMR spectrum (500 MHz, 293 K, CD_3CN) 8.48 (d, $^3J_{HH}$ = 8.5, 6H, bipyH), 8.43 (br s, 6H, ImH), 7.82 7.82 (dd, $^3J_{HH}$ = 8.5, $^3J_{HH}$ = 2.0, 6H, bipyH), 7.63 (d, $^3J_{HH}$ = 2.0, 6H, bipyH), 7.39 (app. t, J_{HH} = 1.8, 7H, ImH), 7.20 (app. t, J_{HH} = 1.9, 6H, ImH), 5.25 (s, 12H, $ArCH_2$), 3.84 (s, 18H, $ImCH_3$); $^{13}C\{^1H\}$ NMR spectrum (126 MHz, 293 K, D_2O; conducted on $[Ru(L_2)_3]Cl_8$ due to solubility reasons); 156.2 (s, bipy), 151.1 (s, bipy), 137.2 (s, Im), 124.7 (s, bipy), 124.5 (s, Im), 122.6 (s, Im), 49.4 (s, $ArCH_2$), 36.4 (s, $ImCH_3$) ppm. ESI-MS *m/z* calcd for $[C_{60}H_{64}N_{18}RuP_6F_{36}]^{2+}$, 1005.1314; found, 1005.1326. IR (ATR): ν_{max} 3169, 3126, 2349, 2324, 1664, 1578, 1564, 1477, 1446, 1425, 1400, 1167, 740, 671, 623, 470 cm^{-1}.

RESULTS AND DISCUSSION

Synthesis. The cationic bipy targets were chosen because they contained one or two imidazolium groups at the 5 and 5′ positions of the diimine. Therefore, the precursors 5-chloromethyl-2,2′-bipyridine and 5,5′-bis-chloromethyl-2,2′-bipyridine were synthesized according to previously reported procedures (via the carboxylic acid, ester, and methyl alcohol intermediates; Section S2.1).[41] The final ligands were obtained from alkylation of the chloromethyl derivatives using *N*-methylimidazole as a reagent and solvent to give the target mono- and dicationic analogues, **L1** and **L2**,[42] in 78% and >99% yield, respectively (Scheme 1). All experimental and characterization details are presented in the Supporting Information.

Despite the ubiquity of $[Ru(bipy)_3]^{2+}$ analogues and their syntheses in the literature,[43] the application of relatively standard complexation procedures in our hands (viz. refluxing EtOH/H_2O mixtures) did not give satisfactory outcomes with the cationic ligands **L1** and **L2**, resulting in incomplete complexation despite extended reaction times. This is presumably due to unfavorable electrostatic repulsion between the incoming ligands and the electropositive ruthenium center. Consequently, more forcing conditions were employed, for example, using refluxing ethylene glycol as a solvent. Application of this protocol to the formation of the tricationic and tetracationic complexes resulted in complete complexation within 3 h, with no evidence of decomposition.

After purification by column chromatography on SiO_2 and anion exchange, $[Ru(bipy)_2(\mathbf{L1})][PF_6]_3$, which has been previously reported and investigated in cell imaging studies,[44] and $[Ru(bipy)_2(\mathbf{L2})][PF_6]_4$ were afforded in yields of 60% and 40%, respectively. The synthesis of the hexacationic derivative

https://doi.org/10.1021/acs.inorgchem.3c02352
Inorg. Chem. 2023, 62, 19446−19456

$[Ru(bipy)(\mathbf{L2})_2][PF_6]_6$ was attempted using a previously utilized two-step route via a $[Ru(\mathbf{L2})_2Cl_2]Cl_4$ intermediate (Scheme 2). In this case, complexation was achieved using

Scheme 2. Attempted Synthesis of the Intermediate Species $[Ru(\mathbf{L2})_2Cl_2]Cl_4$

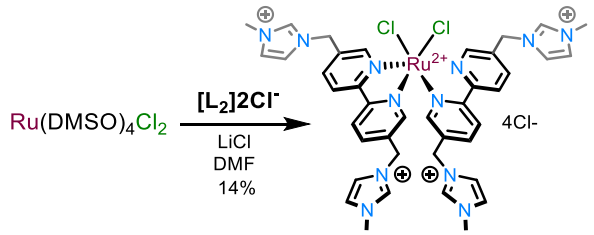

refluxing dimethylformamide (DMF) in the presence of excess LiCl to inhibit the formation of the tris-homoleptic $[Ru(\mathbf{L2})_3]^{8+}$ byproduct.[45] After chromatographic purification, the target compound was isolated, albeit in low yield (14%), and the paucity of isolated compound precluded its use in the next synthetic step.

Therefore, an alternative procedure adapted from Meyer[25] was employed to promote the formation of the desired compound. The reaction of [Ru(*p*-cymene)(bipy)Cl]Cl with ligand **L2** in refluxing ethylene glycol resulted in the total consumption of starting materials, but with the formation of several products (as indicated by ^{1}H NMR spectroscopy), which was ascribed to ligand scrambling and thus related complexes of the general formula $[Ru(bipy)_x(\mathbf{L2})_{3-x}]$. Conversely, the reaction at 120 °C in ethylene glycol resulted in an incomplete reaction, even with extended reaction times. Gratifyingly, the reaction of [Ru(*p*-cymene)(bipy)Cl]Cl with ligand **L2** in refluxing 2-ethoxyethanol produced a single species after 48 h, with no evidence of ligand scrambling at ruthenium. After chromatography on silica and anion exchange, hexacationic $[Ru(bipy)(\mathbf{L2})_2][PF_6]_6$ was isolated in 36% yield. The modest yields of the aforementioned complexes progressively decrease as a function of increasing charge which may be attributed to their elevated affinities to the stationary phase during chromatographic purification. Finally, the synthesis of $[Ru(\mathbf{L2})_3][PF_6]_8$ was achieved using $[Ru(DMSO)_4Cl_2]$ as a starting material and three equivalents of **L2** in refluxing ethylene glycol. In this case, the product was purified by column chromatography of the crude $[Ru(\mathbf{L2})_3]Cl_8$ using Al_2O_3—due to the high affinity of the octacationic homologue when utilizing silica—and anion exchanged thereafter to obtain $[Ru(\mathbf{L2})_3][PF_6]_8$ in 31% yield. The isolation of this final complex matches the record for the most highly charged mononuclear Ru(II) complex reported in the literature.[25]

The complexes were fully characterized using 1D and 2D NMR (298 K, CD_3CN) spectroscopy (^{1}H (Figure 1), ^{13}C, COSY, HSQC, HMBC, ROESY) and mass spectrometry (Figures S17−S32). Complex $[Ru(bipy)_2(\mathbf{L1})][PF_6]_3$ exhibits C_1 symmetry, resulting in the inequivalence of all bipyridine ligands, giving a total of six discrete pyridine moieties. The tetra- and hexacationic complexes $[Ru(bipy)_2(\mathbf{L2})][PF_6]_4$ and $[Ru(bipy)(\mathbf{L2})_2][PF_6]_6$ both display time-averaged C_2 symmetry in solution. In the case of the tetra-cationic derivative, the X′ notation denotes the pyridine fragment which is closest to the imidazolium-functionalized ligand as determined using through-space ^{1}H−^{1}H correlation. Unfortunately, the highly second-order spectrum of $[Ru(bipy)(\mathbf{L_2})_2][PF_6]_6$ prevented the absolute assignment of the unsymmetrical **L2** ligand. In the octacationic congener $[Ru(\mathbf{L2})_3][PF_6]_8$, we observed a time-averaged C_3 species, in agreement with the unfunctionalized parent $[Ru(bipy)_3][PF_6]_2$. Other salient features of the ^{1}H

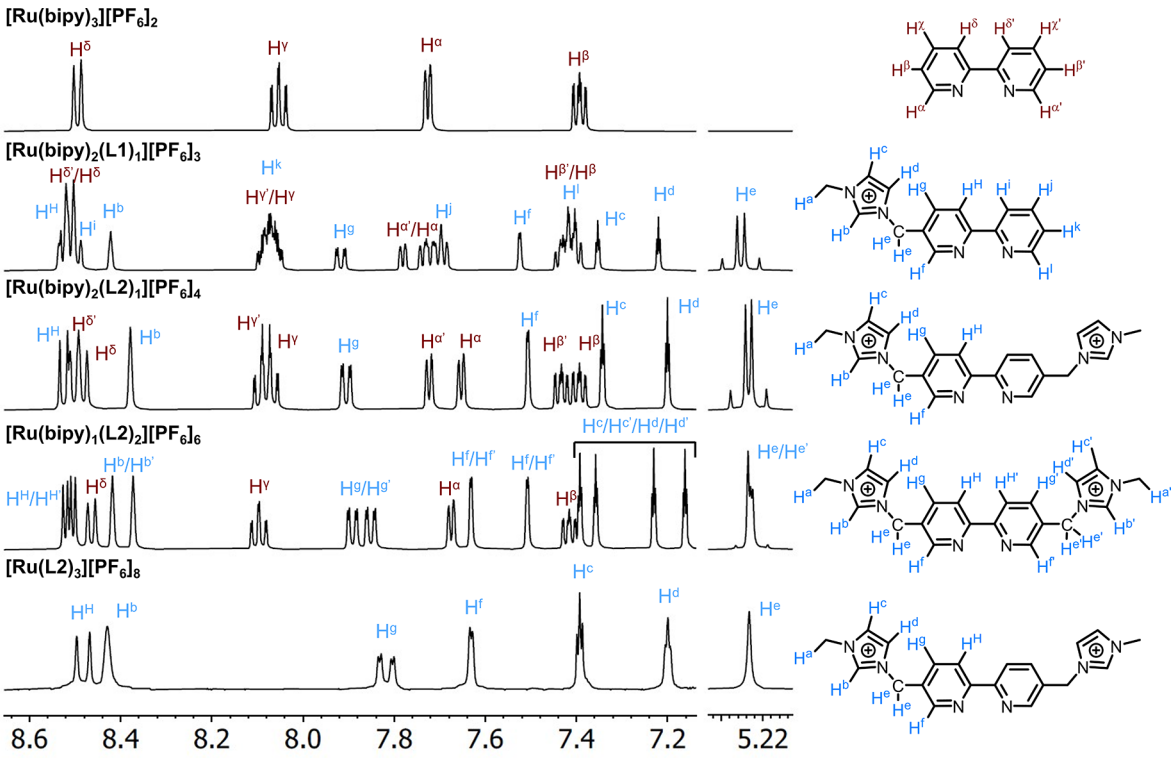

Figure 1. Assignment of ^{1}H NMR spectra (500 MHz, 298 K, CD_3CN) for the family of polycationic Ru(II) complexes.

https://doi.org/10.1021/acs.inorgchem.3c02352
Inorg. Chem. 2023, 62, 19446−19456

NMR spectra are the methylenic CH_2 imidazolium resonances, which—in contrast to the uncoordinated ligands **L1** and **L2**—exhibited diasterotopicity at 298 K. This probably arises from the complexation and thus steric interference from proximate ligand systems, although subtle effects of counteranion ion-packing cannot be ruled out. Interestingly, in the case of $[Ru(bipy)(\mathbf{L2})_2][PF_6]_6$, which displays inequivalence of the two halves of complexed **L2**, one CH_2 resonance appears as a singlet corresponding to fast bond rotation on the NMR time scale, while the other is diastereotopic resulting from slow bond rotation. Due to the resolution of the 2D spectra (298 K, 600 MHz), it was not possible to identify each CH_2 resonance.

Single Crystal X-ray Crystallography. Single crystals of $[Ru(bipy)_2(\mathbf{L2})][PF_6]_4$ suitable for single-crystal X-ray diffraction (SCXRD) analysis (Figure 2, Table S1, Figures S33, 34) were grown from cooling of a concentrated KNO_3/NH_4PF_6 aqueous solution. The compound crystallized in the triclinic $P\bar{1}$ space group with two molecules and the eight hexafluorophosphate anions in the asymmetric unit with no additional solvent present. The three-dimensional network is perpetuated by intermolecular C−H···F hydrogen bonding interactions between the fluorine atoms of the counteranions and polarized C−H bonds in the complex. Mirroring the solution-state behavior, complex $[Ru(bipy)_2(\mathbf{L2})][PF_6]_4$ displays pseudo-C_2 symmetry with an *anti*-arrangement of the flanking methyl-imidazolium groups which hydrogen-bonds intramolecularly to two nested PF_6^- anions, with mean C···F distances of 3.191 Å to the most acidic imidazolium N−CH−N hydrogen. This is augmented by supplementary elongated interactions with the imidazolium CH_3 groups ($(C\cdots F)_{mean}$ = 3.617 Å) and adjacent unfunctionalized bipyridine ligands ($(C\cdots F)_{mean}$ = 3.403 Å). The coordination geometry is largely unchanged from simple heteroleptic ruthenium diimine analogues, with mean $Ru-N_{bipy}$ distances of 2.071 Å and $Ru-N_{L2}$ distances of 2.066 Å (cf. $[Ru(bipy)_2(bipicoline)][PF_6]_2$; $(Ru-N_{bipy})_{mean}$ = 2.065 Å, $(Ru-N_{bipicoline})_{mean}$ = 2.067 Å),[19] indicating that the introduction of the charged imidazolium groups does not significantly alter the ligand field strength of the resultant complex.

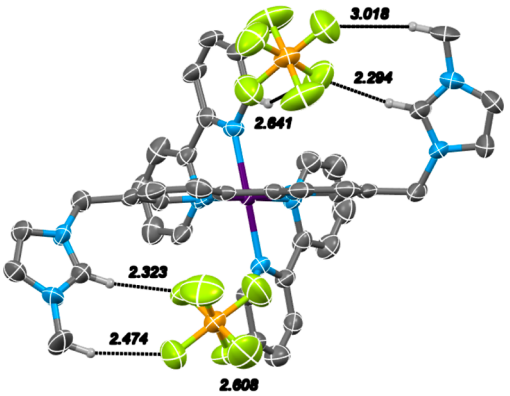

Figure 2. X-ray crystal structure of the $[Ru(bipy)_2(\mathbf{L2})][PF_6]_4$ complex (ellipsoids are plotted at the 50% probability level; non-H-bonding hydrogen atoms and counterions omitted for clarity; CCDC no. 2250505).

Electrochemistry. The electrochemical properties of the family of polycationic ruthenium complexes were explored using cyclic voltammetry in MeCN solution at 1 mM concentration, using $[^nBu_4N][PF_6]$ as the supporting electrolyte (0.1 M) and the Fc/Fc^+ redox couple as a reference (Table 1). All complexes exhibit quasi-reversible or reversible redox waves for both the oxidation and reduction potentials of the metal center and ligand sphere, respectively (Figure S35). The principal feature of the Ru^{II}/Ru^{III} couple is the small variance of the tri- and tetracationic oxidation potentials (E^0) ($[Ru(bipy)_2(\mathbf{L1})][PF_6]_3$ = +0.88 V, $[Ru(bipy)_2(\mathbf{L2})][PF_6]_4$ = 0.91 V) compared to the unsubstituted parent $[Ru(bipy)_3][PF_6]_2$ (+0.89 V), indicating only a small effect of the increase of peripheral charge in the second coordination sphere. For the more highly charged analogues, an increased perturbation is observed, manifested by an increasingly facile one-electron reduction of the Ru^{II} center. For the hexacationic $[Ru(bipy)(\mathbf{L2})_2][PF_6]_6$ complex, E^0 shifts to +0.83 V, while for the octacationic derivative $[Ru(\mathbf{L2})_3][PF_6]_8$, E^0 = +0.80 V. Despite the increased facility of this oxidation process, qualitative observation of the voltammograms indicate that this process became less reversible traversing down the series, which can be reconciled by the decreased stability of the generated Ru^{III} species in solution in close proximity to the multiple pendant cationic imidazolium moieties. Three distinct negative potentials were observed in all cases corresponding to bipyridine reduction of the tris-homoleptic and tris-heteroleptic complexes; imidazolium groups are known to be electrochemically inert within the redox potential window studied.[20] Once again, the reduction waves of $[Ru(bipy)_2(\mathbf{L1})][PF_6]_3$ and $[Ru(bipy)_2(\mathbf{L2})][PF_6]_4$ largely resemble unsubstituted $[Ru(bipy)_3][PF_6]_2$, while we observed the ligand reductions becoming more difficult in the highly charged $[Ru(bipy)(\mathbf{L2})_2][PF_6]_6$ and $[Ru(\mathbf{L_2})_3][PF_6]_8$ complexes. The ease of reduction (cf. $[Ru(bipy)_3][PF_6]_2$) correlates with the overall charge state of the $[Ru(bipy)(\mathbf{L2})_2][PF_6]_6$ and $[Ru(\mathbf{L2})_3][PF_6]_8$ complexes (Δ_{mean} = −0.14 and Δ_{mean} = −0.21, respectively). The observation of more difficult ligand reduction potentials is consistent with the more facile Ru^{II}/Ru^{III} redox couples, although this is counterintuitive since one might expect the inverse upon introducing multiple positive charges close to the metal center. We tentatively ascribe this behavior to the presence of the multiple ion-paired hexafluorophosphate anions, which may stabilize the formation of Ru^{III} and thus destabilize the reduction of the bipyridine ligands. Indeed, the magnitude of the shift of the redox process is larger for the ligand reduction potentials and can be rationalized in the relative distance from the charged imidazolium groups (vide supra; SCXRD). Ligand reduction, and its proximity to the imidazolium moieties, is more susceptible to inductive charged effects from the hexafluorophosphate anions, which are ion-paired with the imidazolium groups, when compared to the Ru^{II}/Ru^{III} oxidation.

Table 1. Electrochemical Oxidation and Reduction Potentials of the Family of Complexes

complex	RuII/III	$bipy^{0/-1}$	$bipy^{-1/-2}$	$bipy^{-2/-3}$
$[Ru(bipy)_3][PF_6]_2$	0.89(200)	−1.76(161)	−1.94(180)	−2.18(200)
$[Ru(bipy)_2(\mathbf{L1})][PF_6]_3$	0.88(120)	−1.75(100)	−1.94(113)	−2.20(115)
$[Ru(bipy)_2(\mathbf{L2})][PF_6]_4$	0.91(120)	−1.71(130)	−1.93(100)	−2.21(130)
$[Ru(bipy)(\mathbf{L2})_2][PF_6]_6$	0.83(160)	−1.83(140)	−2.08(220)	−2.34(203)
$[Ru(\mathbf{L2})_3][PF_6]_8$	0.80(209)	−1.95(130)	−2.15(190)	−2.41(187)

https://doi.org/10.1021/acs.inorgchem.3c02352
Inorg. Chem. 2023, 62, 19446−19456

Table 2. Absorption and Photoluminescence Data for the Family of Polycationic Complexes[a,b]

complex	λ_{MLCT}/nm (ε/M^{-1} cm^{-1})	λ_{em}/nm[c]	τ/ns[d]	Degas τ/ns[d]	Φ_{Ru}	Degas Φ_{Ru}	$k_r/10^4$ s^{-1}	$k_{nr}/10^5$ s^{-1}
$[Ru(bipy)_3][PF_6]_2$	450 (15,300)	610	157	867	0.018[47]	0.095[48]		
$[Ru(bipy)_2(\mathbf{L1})][PF_6]_3$	450 (14,000)	633	218	907	0.017[e]	0.069[f]	0.76	10.3
$[Ru(bipy)_2(\mathbf{L2})][PF_6]_4$	452 (13,100)	654	236	568	0.014[e]	0.049[f]	0.86	16.4
$[Ru(bipy)(\mathbf{L2})_2][PF_6]_6$	456 (12,300)	643	331	744	0.018[e]	0.041[f]	0.55	12.9
$[Ru(\mathbf{L2})_3][PF_6]_8$	456 (12,500)	632	362	841	0.021[e]	0.054[f]	0.64	11.2

[a]All measurements were obtained in MeCN at 293 K. [b]1×10^{-5} M. [c]λ_{ex} = 450 nm. [d]Observed lifetime, λ_{ex} = 295 nm. [e]Using $[Ru(bipy)_3][PF_6]_2$ in aerated MeCN as a reference (Φ = 0.018).[48] [f]Using $[Ru(bipy)_3][PF_6]_2$ in degassed MeCN as a reference (Φ = 0.095), errors are estimated at 15%.[48] Estimates of k_r and k_{nr} using $k_r = \Phi/\tau$ and $k_{nr} = (1 - \Phi)/\tau$.

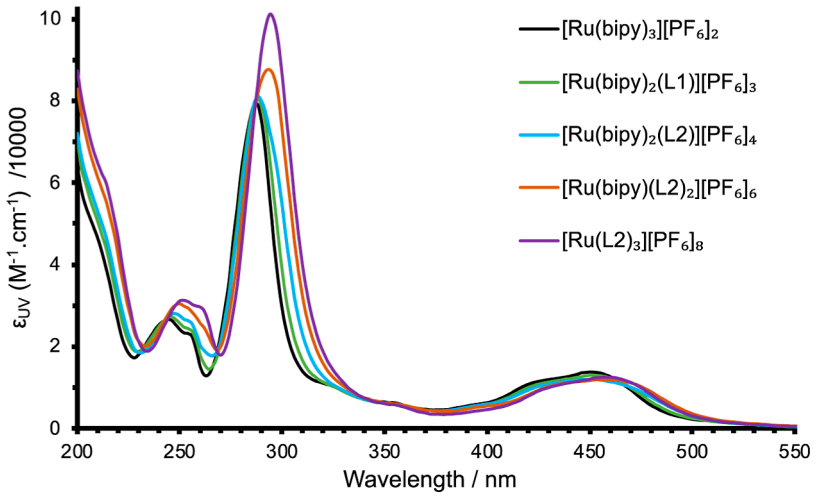

Figure 3. UV−vis absorption spectra for the family of polycationic ruthenium complexes (MeCN).

Photophysical Properties of the Complexes. The UV−vis absorption data for all complexes were obtained in aerated acetonitrile and are presented in Table 2 and Figure 3. The two notable regions are high-intensity UV absorptions corresponding to allowed $\pi \rightarrow \pi^*$ transitions and weaker absorptions in the visible region, around 450 nm, due to spin-allowed ^{1}MLCT absorptions. The tri- and tetracationic complexes displayed high energy absorptions at 288 nm ($\varepsilon \approx$ 82,000 M^{-1} cm^{-1}), which are comparable to that of $[Ru(bipy)_3][PF_6]_2$. For the hexacationic complex, this feature is slightly shifted to lower energy (294 nm), but with an increased molar absorptivity (88,000 M^{-1} cm^{-1}), while the octacationic derivative displays the same maximum but again with a concomitantly higher absorption coefficient (101,300 M^{-1} cm^{-1}). The ^{1}MLCT transition displayed only a minor variation in the wavelength position (450−456 nm), with the associated molar absorptivity slightly decreasing down the series of complexes. The shape of the MLCT band envelope is consistent with previous descriptions that describe the vibronic progressions associated with the transition.[46] These results demonstrate that the pendant imidazolium groups induce a small effect on the ground state absorption properties of the Ru(II) complexes.

The corresponding photoluminescence spectra of the complexes were initially recorded in aerated MeCN. All compounds were found to be luminescent upon excitation at 450 nm (i.e., directly into the ^{1}MLCT absorption band), showing a broad featureless emission maxima at ca. 630 nm which clearly corresponds to ^{3}MLCT emission. The effect of the imidazolium groups upon the excited state characteristics was found to be more pronounced than for ground state absorption (Figure 4). Introduction of one imidazolium group (i.e., $[Ru(bipy)_2(\mathbf{L1})][PF_6]_3$) induced a bathochromic shift of

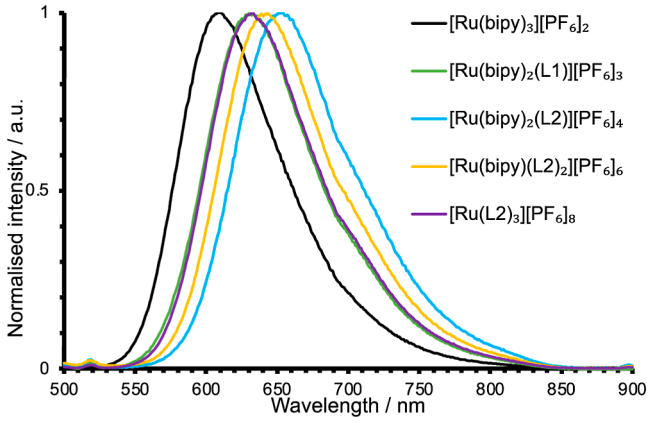

Figure 4. Normalized emission spectra for the family of polycationic ruthenium complexes (293 K, aerated MeCN, 10^{-5} M).

23 nm vs unfunctionalized $[Ru(bipy)_3][PF_6]_2$. This was also observed for the tetracationic $[Ru(bipy)_2(\mathbf{L2})][PF_6]_3$ complex (λ_{em} = 654 nm, $\Delta\lambda_{MLCT}$ = 44 nm), with the effect of the second imidazolium group being roughly additive. Strikingly, the hexacationic complex did not continue this trend (λ_{em} = 643 nm, $\Delta\lambda_{MLCT}$ = 33 nm), displaying a relative hypsochromic shift vs the tetracationic complex. Finally, the emission maximum of $[Ru(\mathbf{L2})_3][PF_6]_8$ (λ_{em} = 632 nm, $\Delta\lambda_{MLCT}$ = 21 nm) again shifted to higher energy.

In addition to the acquisition of experimental data, supporting density functional theory (DFT) results showed that all of the transitions observed within the range of 250 nm < λ < 700 nm are predicted to be strongly MLCT in character (the calculated Kohn−Sham molecular orbitals are shown in

https://doi.org/10.1021/acs.inorgchem.3c02352
Inorg. Chem. 2023, 62, 19446−19456

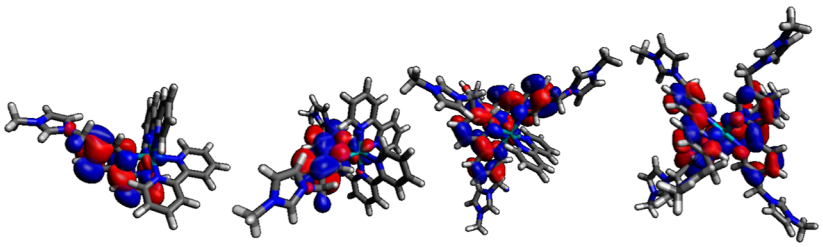

Figure 5. Calculated Kohn–Sham LUMOs for (left to right) $[Ru(bipy)_2(\mathbf{L1})]^{3+}$, $[Ru(bipy)_2(\mathbf{L2})]^{4+}$, $[Ru(bipy)(\mathbf{L2})_2]^{6+}$, and $[Ru(\mathbf{L2})_3]^{6+}$.

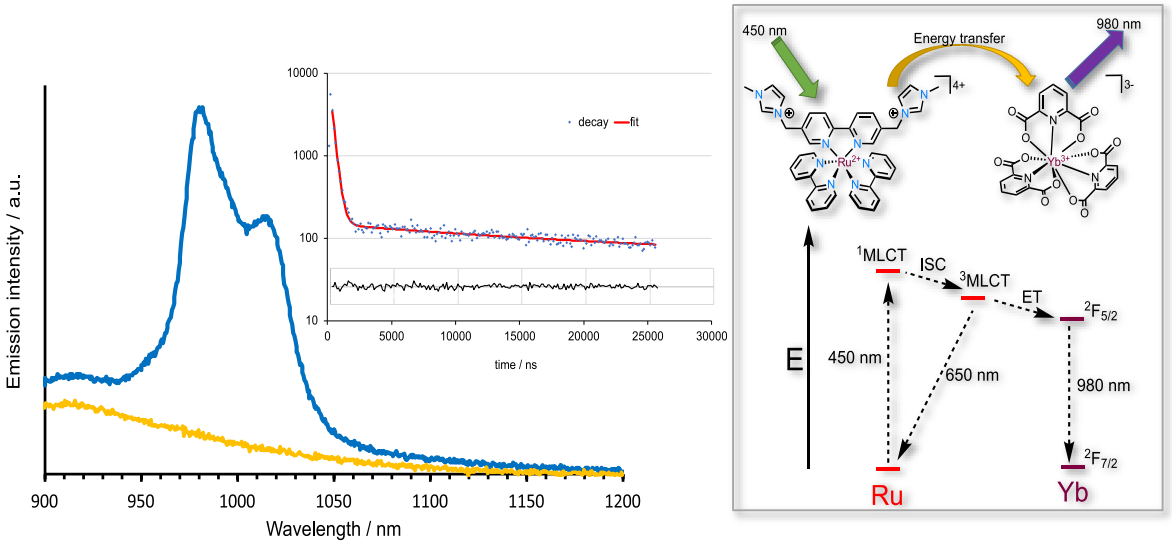

Figure 6. Comparison of the NIR emission spectra of $[Ru(bipy)_3]^{2+}$ (orange) and $[Ru(bipy)_2(\mathbf{L2})]^{4+}$ (blue) solutions in the presence of 2 eq $[Yb(dpa)_3]^{3-}$ (293 K, aerated D_2O, 10^{-5} M Ru(II) complex, λ_{ex} = 450 nm). Fitted decay (residual errors shown) for $[Ru(bipy)_2(\mathbf{L2})]^{4+}$ in the presence of 2 eq $[Yb(dpa)_3]^{3-}$ (293 K, aerated D_2O, 10^{-5} M, λ_{ex} = 355 nm, λ_{em} = 980 nm). The obtained lifetimes were 0.3 μs (31% relative weighting) and 21.9 μs (69%). The proposed photophysical pathways are shown inset.

Tables S2–S5). In all cases, the transitions involved in the absorption bands observed within this window arise from occupied orbitals with 70% or greater Ru(4d) character, and with unoccupied character <10% Ru(4d). TD-DFT calculations show a qualitative agreement with the luminescence band positions, but they appear to greatly overpredict the wavelength shifts in the absorption band positions (Tables S6–S10). However, the longest wavelength absorber/emitter is correctly predicted to be the $[Ru(bipy)_2(\mathbf{L2})]^{4+}$ complex, seemingly due to a relative reduction in the energy of the LUMO.

In each complex, the strongest transitions are predicted where there are significant HOMO−2/LUMO contributions, and therefore, the influence of the position of the LUMO is probably of great importance. For $[Ru(bipy)_2(\mathbf{L1})]^{3+}$ and $[Ru(bipy)_2(\mathbf{L2})]^{4+}$, the calculations predict that the LUMO is primarily localized on **L1**/**L2**. This is not surprising as this affords a more nonzero transition probability based on orbital overlap arguments, with low-lying **L1**/**L2**-centered unoccupied orbitals, particularly given the high localization of many of the occupied orbitals on the metal center. For complexes $[Ru(bipy)(\mathbf{L2})_2]^{6+}$ and $[Ru(\mathbf{L2})_3]^{8+}$, the LUMOs may become delocalized across multiple **L2** ligands (Figure 5), perhaps explaining the trend noted in the experimental data.

Time-resolved photophysical measurements yielded the emission lifetimes, which increased down the series from 218 to 362 ns (cf. 157 ns for $[Ru(bipy)_3][PF_6]_2$) in aerated MeCN, possibly indicating that quenching in the oxygenated solvent may be inhibited by increasing the number of imidazolium moieties. Quantum yield (QY) measurements were also conducted in aerated MeCN and also showed a break in behavior demonstrated by the λ_{em} data: in general, the quantum yield reduced up to the tetracationic complex (Φ = 0.014) and thereafter recovered down the series to eventually surpass unfunctionalized $[Ru(bipy)_3][PF_6]_2$ in the case of $[Ru(\mathbf{L2})_3][PF_6]_8$ (Φ = 0.021). The spectroscopic measurements were repeated in deoxygenated MeCN. First, the lifetimes were increased in all cases emphasizing the ^{3}MLCT nature of the phosphorescence. The degassed lifetime and QY data now broadly replicate the same trend: a general reduction in values to $[Ru(bipy)_2(\mathbf{L2})][PF_6]_4$ and then a subsequent increase to $[Ru(\mathbf{L2})_3][PF_6]_8$. To probe this further, the relative rates of radiative and nonradiative decay were calculated and show that the values of the nonradiative decay constant (k_{nr}) correlate with the Energy Gap Law. Thus, the longest wavelength tetracationic emitter has the highest value of k_{nr}.

Finally, we were interested in the potential utility of these polycationic Ru(II) complexes in further optoelectronic applications. Our hypothesis was that the increase in positive charge could be exploited in the electrostatic assembly of photoactive ion pairs. In particular, we hypothesized that the use of an anionic lanthanide complex might permit energy transfer from a Ru(II)-based donor. Therefore, polyanionic $[Yb(dpa)_3]^{3-}$ (where dpa = pyridine-2,6-dicarboxylic acid) was identified as an ideal candidate. Initially, ^{1}H NMR studies were undertaken whereby $[Yb(dpa)_3]^{3-}$ was added to a solution of

https://doi.org/10.1021/acs.inorgchem.3c02352
Inorg. Chem. 2023, 62, 19446−19456

$[Ru(bipy)_2(\mathbf{L2})]^{4+}$ in 0.1 M KNO_3 D_2O solution (Figure S36). Addition of the paramagnetic Yb(III) complex induced small perturbations ($\Delta\delta$ < 0.2 ppm) of the bipyridine resonances of $[Ru(bipy)_2(\mathbf{L2})]^{4+}$, although their broad nature precludes absolute assignment. More strikingly, the peripheral methylenic and methyl resonances exhibit broadening and downfield shifts of 1.09 and 0.68 ppm, respectively, indicating interactions between the two complex units.

Photoluminescent studies were then undertaken to probe the photophysical attributes of the solution mixture. First, an aerated D_2O solution of the parent unfunctionalized $[Ru(bipy)_3]^{2+}$ was measured in the presence of 2 eq $[Yb(dpa)_3]^{3-}$. An excitation wavelength of 450 nm was used and is selective for the ^{1}MLCT band of the Ru(II) complex (note that $[Yb(dpa)_3]^{3-}$ does not absorb >320 nm). No characteristic signal for Yb(III)-based emission was noted, with only the weak tail of the ^{3}MLCT band evident in the NIR window. We repeated the experiment using $[Ru(bipy)_2(\mathbf{L2})]^{4+}$ which was chosen due to its high charge and also its significantly red-shifted ^{3}MLCT emission wavelength when compared to $[Ru(bipy)_3]^{2+}$ (654 nm vs 610 nm) which should maximize spectral overlap with Yb(III). Utilizing the more highly cationic $[Ru(bipy)_2(\mathbf{L2})]^{4+}$ produced a remarkably different result: the characteristic emission profile of Yb(III) was immediately evident with a strong structured emission ca. 980 nm with a shoulder at 1020 nm corresponding to the Stark-split sublevels of the $^2F_{5/2} \rightarrow {}^2F_{7/2}$ transition (Figure 6). From the baseline profile, it is clear that the Yb(III) emission is superimposed upon the low energy tail of the ^{3}MLCT band which was corroborated through time-resolved NIR measurements (λ_{em} = 980 nm) that revealed a decay profile (Figure 6) that fitted well to a biexponential function giving two distinct lifetime values of 0.3 (further refined to 392 ns using a shorter 1 μs window for the analysis) and 21.9 μs. Since $[Yb(dpa)_3]^{3-}$ has a reported lifetime of 39 μs in D_2O,[48] the measured values are attributed to the coemission of the residual ^{3}MLCT signal and the Yb-centered emission, respectively. Unfortunately, the biexponential character of the decay at 980 nm prevented us from extracting a rise time to the Yb(III) emission. Therefore, these measurements establish that Ru → Yb energy transfer, which we assume proceeds via a Förster mechanism, must be feasible in electrostatically assembled mixtures of ion-paired complexes in solution. Given that this behavior was not observed for $[Ru(bipy)_3]^{2+}$, the presence of additional charge and/or pendant hydrogen-bonding interactions may be vital in the observation of Ru → Yb energy transfer.

CONCLUSIONS

This study has shown that a variety of synthetic approaches can be employed to isolate a series of cationic Ru(II) polypyridine-type complexes with overall charges systematically varying from +2 to +8; the octa-cationic complex match the highest reported magnitude of charge in the literature for Ru(II) species. Each of the complexes was demonstrated to be luminescent from a ^{3}MLCT emitting state (610−654 nm). The interesting trend in λ_{em} shows a maximum value for the +4 species before hypsochromically shifting for +6 and +8, which may indicate the shielding effects of ion pairing in solution; degassed lifetime and quantum yield measurements support this trend. The solution state photophysical utility of polycationic Ru(II) complexes was exploited in experiments using a polyanionic Yb(III) complex. These studies show that energy transfer and subsequent sensitization of the Yb(III) excited state are possible in free solution resulting in NIR emission from Yb(III). This implies that electrostatically driven ion pairing (perhaps supported by H-bonding interactions) is possible in solution and can be used to facilitate photophysical phenomena, such as through space energy transfer mechanisms. Further detailed photophysical studies are required to expand the range of measurements using different combinations of polycationic Ru(II) donors and $[Ln(dpa)_3]^{3-}$ acceptors. Such studies should allow for a more detailed appreciation of the importance of charge and the efficiencies of energy transfer in sensitized pairings.

More broadly, the development of mixed ligand complexes of Ru(II) and the study of localized versus delocalized excited states may have importance in areas of study focused on ultrafast electron injection at semiconductor interfaces as noted elsewhere. An investigation of interligand electron transfer (electron hopping) within excited state polycationic Ru(II) species could be particularly relevant.

ASSOCIATED CONTENT

Supporting Information

The Supporting Information is available free of charge at https://pubs.acs.org/doi/10.1021/acs.inorgchem.3c02352.

^{1}H and ^{13}C NMR, and ESI-HRMS spectra for ligands and corresponding complexes; single-crystal X-ray crystallography; cyclic voltammetry; and density functional theory (PDF)

Accession Codes

CCDC 2250505 contains the supplementary crystallographic data for this paper. These data can be obtained free of charge via www.ccdc.cam.ac.uk/data_request/cif, or by emailing data_request@ccdc.cam.ac.uk, or by contacting The Cambridge Crystallographic Data Centre, 12 Union Road, Cambridge CB2 1EZ, UK; fax: +44 1223 336033.

AUTHOR INFORMATION

Corresponding Authors

Richard C. Knighton − *School of Chemistry, Main Building, Cardiff University, Cardiff CF10 3AT Cymru/Wales, U.K.;* Present Address: R.C.K. University of Southampton, Southampton, Hampshire, UK SO17 1BJ; orcid.org/0000-0002-0336-3718; Email: R.C.Knighton@soton.ac.uk

Simon J. A. Pope − *School of Chemistry, Main Building, Cardiff University, Cardiff CF10 3AT Cymru/Wales, U.K.;* orcid.org/0000-0001-9110-9711; Email: popesj@cardiff.ac.uk

Author

Joseph M. Beames − *School of Chemistry, University of Birmingham, Birmingham B152TT, England;* orcid.org/0000-0002-5508-8236

Complete contact information is available at: https://pubs.acs.org/10.1021/acs.inorgchem.3c02352

Notes

The authors declare no competing financial interest.

ACKNOWLEDGMENTS

Financial support from the Leverhulme Trust (RPG-2021-003) is gratefully acknowledged. We acknowledge the use of the EPSRC-funded Physical Sciences Data-science Service

hosted by the University of Southampton and STFC under grant no. EP/S020357/1.

REFERENCES

(1) Han, W.-K.; Liu, Y.; Yan, X.; Jiang, Y.; Zhang, J.; Gu, Z.-G. Integrating Light-Harvesting Ruthenium(II)-Based Units into Three-Dimensional Metal Covalent Organic Frameworks for Photocatalytic Hydrogen Evolution. *Angew. Chem., Int. Ed.* **2022**, *61*, No. e202208791.

(2) Yong, C.-K.; Parkinson, P.; Kondratuk, D. V.; Chen, W.-H.; Stannard, A.; Summerfield, A.; Sprafke, J. K.; O'Sullivan, M. C.; Beton, P. H.; Anderson, H. L.; Herz, L. M. Ultrafast Delocalization of Excitation in Synthetic Light-Harvesting Nanorings. *Chem. Sci.* **2015**, *6*, 181−189.

(3) Cesana, P. T.; Li, B. X.; Shepard, S. G.; Ting, S. I.; Hart, S. M.; Olson, C. M.; Martinez Alvarado, J. I.; Son, M.; Steiman, T. J.; Castellano, F. N.; Doyle, A. G.; MacMillan, D. W. C.; Schlau-Cohen, G. S. A Biohybrid Strategy for Enabling Photoredox Catalysis with Low-Energy Light. *Chem* **2022**, *8*, 174−185.

(4) Sathish, V.; Ramdass, A.; Velayudham, M.; Lu, K.-L.; Thanasekaran, P.; Rajagopal, S. Development of Luminescent Sensors Based on Transition Metal Complexes for the Detection of Nitroexplosives. *Dalton Trans.* **2017**, *46*, 16738−16769.

(5) Knighton, R. C.; Dapin, S.; Beer, P. D. Luminescent Anion Sensing by Transition-Metal Dipyridylbenzene Complexes Incorporated into Acyclic, Macrocyclic and Interlocked Hosts. *Chem.—Eur. J.* **2020**, *26*, 5288−5296.

(6) Bharmoria, P.; Bildirir, H.; Moth-Poulsen, K. Triplet-Triplet Annihilation Based near Infrared to Visible Molecular Photon Upconversion. *Chem. Soc. Rev.* **2020**, *49*, 6529−6554.

(7) (a) Zhao, J.; Wu, W.; Sun, J.; Guo, S. Triplet photosensitizers: from molecular design to applications. *Chem. Soc. Rev.* **2013**, *42*, 5323−5351. (b) Elgar, C. E.; Otaif, H. Y.; Zhang, X.; Zhao, J.; Horton, P. N.; Coles, S. J.; Beames, J. M.; Pope, S. J. A. Iridium(III) Sensitisers and Energy Upconversion: The Influence of Ligand Structure upon TTA-UC Performance. *Chem.—Eur. J.* **2021**, *27*, 3427−3439.

(8) Knighton, R. C.; Soro, L. K.; Thor, W.; Strub, J.-M.; Cianférani, S.; Mély, Y.; Lenertz, M.; Wong, K.-L.; Platas-Iglesias, C.; Przybilla, F.; Charbonnière, L. J. Upconversion in a d-f [RuYb3] Supramolecular Assembly. *J. Am. Chem. Soc.* **2022**, *144*, 13356−13365.

(9) (a) Poynton, F. E.; Bright, S. A.; Blasco, S.; Williams, D. C.; Kelly, J. M.; Gunnlaugsson, T. The development of ruthenium(II) polypyridyl complexes and conjugates for: In vitro cellular and in vivo applications. *Chem. Soc. Rev.* **2017**, *46*, 7706−7756. (b) Shum, J.; Leung, P.-K.; Lo, K. W. Luminescent Ruthenium(II) Polypyridine complexes for a wide variety of biomolecular and cellular applications. *Inorg. Chem.* **2019**, *58*, 2231−2247.

(10) (a) Li, J.; Chen, T. Transition metal complexes as photosensitizers for integrated cancer theranostic applications. *Coord. Chem. Rev.* **2020**, *418*, 213355. (b) Saeed, H. K.; Sreedharan, S.; Jarman, P. J.; Archer, S. A.; Fairbanks, S. D.; Foxon, S. P.; Auty, A. J.; Chekulaev, D.; Keane, T.; Meijer, A. J. H. M.; Weinstein, J. A.; Smythe, C. G. W.; Bernardino de la Serna, J.; Thomas, J. A. Making the Right Link to Theranostics: The Photophysical and Biological Properties of Dinuclear RuII-ReI Dppz Complexes Depend on Their Tether. *J. Am. Chem. Soc.* **2020**, *142*, 1101−1111.

(11) He, L.; Tan, C.-P.; Ye, R.-R.; Zhao, Y.-Z.; Liu, Y.-H.; Zhao, Q.; Ji, L.-N.; Mao, Z.-W. Theranostic Iridium(III) Complexes as One- and Two-Photon Phosphorescent Trackers to Monitor Autophagic Lysosomes. *Angew. Chem., Int. Ed.* **2014**, *53*, 12137−12141.

(12) (a) Karges, J.; Kuang, S.; Maschietto, F.; Blacque, O.; Ciofini, I.; Chao, H.; Gasser, G. Rationally Designed Ruthenium Complexes for 1- and 2-Photon Photodynamic Therapy. *Nat. Commun.* **2020**, *11*, 3262. (b) Martinez-Alonso, M.; Gasser, G. Ruthenium polypyridyl complex-containing bioconjugates. *Coord. Chem. Rev.* **2021**, *434*, 213736.

(13) Wenger, O. S. Photoactive Complexes with Earth-Abundant Metals. *J. Am. Chem. Soc.* **2018**, *140*, 13522−13533.

(14) For example: (a) Bruns, C. J.; Fujita, D.; Hoshino, M.; Sato, S.; Stoddart, J. F. D.; Fujita, M. Emergent Ion-Gated Binding of Cationic Host-Guest Complexes within Cationic M12L24 Molecular Flasks. *J. Am. Chem. Soc.* **2014**, *136*, 12027−12034. (b) Wang, X.-Y.; Sevov, S. C. Hydrogen-Bonded Host Frameworks of Cationic Metal Complexes and Anionic Disulfonate Linkers: Effects of the Guest Molecules and the Charge of the Metal Complex. *Chem. Mater.* **2007**, *19*, 4906−4912.

(15) For example: (a) Sitze, M. S.; Schreiter, E. R.; Patterson, E. V.; Freeman, R. G. Ionic Liquids Based on $FeCl_3$ and $FeCl_2$. Raman Scattering and ab Initio Calculations. *Inorg. Chem.* **2001**, *40*, 2298−2304. (b) Chand, D.; Farooq, M. Q.; Pathak, A. K.; Li, J.; Smith, E. A.; Anderson, J. L. Magnetic ionic liquids based on transition metal complexes with N-alkylimidazole ligands. *New J. Chem.* **2019**, *43*, 20−23.

(16) Macchioni, A. Ion pairing in transition-metal organometallic chemistry. *Chem. Rev.* **2005**, *105*, 2039−2074.

(17) Komor, A. C.; Barton, J. K. The path for metal complexes to a DNA target. *Chem. Commun.* **2013**, *49*, 3617−3630.

(18) For example: (a) Owen, T.; Butler, A. Metallosurfactants of bioinorganic interest: Coordination-induced self assembly. *Coord. Chem. Rev.* **2011**, *255*, 678−687. (b) Griffiths, P. C.; Fallis, I. A.; Chuenpratoom, T.; Watanesk, R. Metallosurfactants: interfaces and micelles. *Adv. Colloid Interface Sci.* **2006**, *122*, 107−117. (c) Donner, A.; Trepka, B.; Theiss, S.; Immler, F.; Traber, J.; Polarz, S. NHC-Metallosurfactants as Active Polymerization Catalysts. *Langmuir* **2019**, *35*, 16514−16520.

(19) Puckett, C. A.; Ernst, R. J.; Barton, J. K. Exploring the Cellular Accumulation of Metal Complexes. *Dalton Trans.* **2010**, *39*, 1159−1170.

(20) Constable, E. C.; Housecroft, C. E. The early years of 2,2'-bipyridine - a ligand in its own lifetime. *Molecules* **2019**, *24*, 3951.

(21) (a) Willink, H. D. T., Jr; Wibaut, J. P. The preparation of 2: 2′-dipyridyl and some of its derivatives. *Recl. Trav. Chim. Pays-Bas* **1935**, *54*, 275−283. (b) Smith, C. R. Skraup's reaction applied to the phenylenediamines. Preparation of the phenanthrolines and related bipyridyls. *J. Am. Chem. Soc.* **1930**, *52*, 397−403.

(22) Gillaizeau-Gauthier, I.; Odobel, F.; Alebbi, M.; Argazzi, R.; Costa, E.; Bignozzi, C. A.; Qu, P.; Meyer, G. J. Phosphonate-Based Bipyridine Dyes for Stable Photovoltaic Devices. *Inorg. Chem.* **2001**, *40*, 6073−6079.

(23) (a) Charbonnière, L. J.; Weibel, N.; Ziessel, R. F. 5'-Substituted-6-Carboxylic-2,2'-Bipyridine Acid: A Pivotal Architecton for Building Preorganized Ligands. *J. Org. Chem.* **2002**, *67*, 3933−3936. (b) Forato, F.; Belhboub, A.; Monot, J.; Petit, M.; Benoit, R.; Sarou-Kanian, V.; Fayon, F.; Jacquemin, D.; Queffelec, C.; Bujoli, B. Phosphonate-Mediated Immobilization of Rhodium/Bipyridine Hydrogenation Catalysts. *Chem.—Eur. J.* **2018**, *24*, 2457−2465.

(24) Karges, J.; Kuang, S.; Maschietto, F.; Blacque, O.; Ciofini, I.; Chao, H.; Gasser, G. Rationally Designed Ruthenium Complexes for 1- and 2-Photon Photodynamic Therapy. *Nat. Commun.* **2020**, *11*, 3262.

(25) Swords, W. B.; Li, G.; Meyer, G. J. Iodide Ion Pairing with Highly Charged Ruthenium Polypyridyl Cations in CH_3CN. *Inorg. Chem.* **2015**, *54*, 4512−4519.

(26) Gao, F.; Chen, X.; Wang, J.-Q.; Chen, Y.; Chao, H.; Ji, L.-N. In Vitro Transcription Inhibition by Ruthenium(II) Polypyridyl Complexes with Electropositive Ancillary Ligands. *Inorg. Chem.* **2009**, *48*, 5599−5601.

(27) Klink, S. I.; Keizer, H.; van Veggel, F. C. J. M. Transition Metal Complexes as Photosensitizers for Near-Infrared Lanthanide Luminescence. *Angew. Chem., Int. Ed.* **2000**, *39*, 4319−4321.

(28) (a) Parker, D.; Williams, J. A. G. Getting excited about lanthanide complexation chemistry. *J. Chem. Soc., Dalton Trans.* **1996**, 3613−3628. (b) Bunzlie, J.-C. G. Lanthanide Luminescence for Biomedical Analyses and Imaging. *Chem. Rev.* **2010**, *110*, 2729−2755. (c) Faulkner, S.; Pope, S. J. A.; Burton-Pye, B. P. Lanthanide complexes for luminescence imaging applications. *Appl. Spectrosc. Rev.*

https://doi.org/10.1021/acs.inorgchem.3c02352
Inorg. Chem. 2023, 62, 19446−19456

2005, *40*, 1−31. (d) Amoroso, A. J.; Pope, S. J. A. Using lanthanide ions in molecular bioimaging. *Chem. Soc. Rev.* **2015**, *44*, 4723−4742.
(29) (a) Faulkner, S.; Natrajan, L. S.; Perry, W. S.; Sykes, D. Sensitised luminescence in lanthanide containing arrays and d-f hybrids. *Dalton Trans.* **2009**, 3890−3899. (b) Ward, M. D. Transition-metal sensitised near-infrared luminescence from lanthanides in d-f heteronuclear arrays. *Coord. Chem. Rev.* **2007**, *251*, 1663−1677.
(30) (a) Aboshyan-Sorgho, L.; Nozary, H.; Aebischer, A.; Bunzli, J.-C.; Morgantini, P.-Y.; Kittilstved, K. R.; Hauser, A.; Eliseeva, S. V.; Petoud, S.; Piguet, C. Optimizing Millisecond Time Scale Near-Infrared Emission in Polynuclear Chrome(III)-Lanthanide(III) Complexes. *J. Am. Chem. Soc.* **2012**, *134*, 12675−12684. (b) Pope, S. J. A.; Coe, B. J.; Faulkner, S.; Laye, R. H. Metal-to-ligand charge-transfer sensitisation of near-infrared emitting lanthanides in trimetallic arrays M2Ln (M = Ru, Re or Os; Ln = Nd, Er or Yb). *Dalton Trans.* **2005**, 1482−1490. (c) Sénéchal-David, K.; Pope, S. J. A.; Quinn, S.; Faulkner, S.; Gunnlaugsson, T. Sensitized Near-Infrared Lanthanide Luminescence from Nd(III)- and Yb(III)-Based Cyclen-Ruthenium Coordination Conjugates. *Inorg. Chem.* **2006**, *45*, 10040−10042. (d) Davies, G. M.; Pope, S. J. A.; Adams, H.; Faulkner, S.; Ward, M. D. Structural and Photophysical Properties of Coordination Networks Combining $[Ru(bipy)(CN)_4]^{2-}$ Anions and Lanthanide-(III) Cations: Rates of Photoinduced Ru-to-Lanthanide Energy Transfer and Sensitized Near-Infrared Luminescence. *Inorg. Chem.* **2005**, *44*, 4656−4665. (e) Herrera, J.-M.; Pope, S. J. A.; Meijer, A. J. H. M.; Easun, T. L.; Adams, H.; Alsindi, W. Z.; Sun, X.-Z.; George, M. W.; Faulkner, S.; Ward, M. D. Photophysical and Structural Properties of Cyanoruthenate Complexes of Hexaazatriphenylene. *J. Am. Chem. Soc.* **2007**, *129*, 11491−11504. (f) Shavaleev, N. M.; Pope, S. J. A.; Bell, Z. R.; Faulkner, S.; Ward, M. D. Visible-light sensitisation of near-infrared luminescence from Yb(iii), Nd(iii) and Er(iii) complexes of 3,6-bis(2-pyridyl)tetrazine. *Dalton Trans.* **2003**, 808−814. (g) Lazarides, T.; Adams, H.; Sykes, D.; Faulkner, S.; Calogero, G.; Ward, M. D. Heteronuclear bipyrimidine-bridged Ru-Ln and Os-Ln dyads: low-energy 3MLCT states as energy-donors to Yb(iii) and Nd(iii). *Dalton Trans.* **2008**, 691−698. (h) Jones, J. E.; Jenkins, R. L.; Hicks, R. S.; Hallett, A. J.; Pope, S. J. A. Water-soluble, luminescent iridium(III)-ytterbium(III) complexes using dipyrido[3,2-a:2 ',3 '-c] phenazine derivatives as bridging units. *Dalton Trans.* **2012**, *41*, 10372−10381. (i) Shavaleev, N. M.; Moorcraft, L. P.; Pope, S. J. A.; Bell, Z. R.; Faulkner, S.; Ward, M. D. Sensitised near-infrared emission from lanthanides using a covalently-attached Pt(ii) fragment as an antenna group. *Chem. Commun.* **2003**, 1134−1135. (j) Li, L.; Zhang, S.; Xu, L.; Chen, Z.-N.; Luo, J. Highly sensitized near-infrared luminescence in Ir-Ln heteronuclear coordination polymers via light-harvesting antenna of Ir(iii) unit. *J. Mater. Chem. C* **2014**, *2*, 1698−1703.
(31) Pope, S. J. A.; Coe, B. J.; Faulkner, S.; Bichenkova, E. V.; Yu, X.; Douglas, K. T. Self-Assembly of Heterobimetallic d-f Hybrid Complexes: Sensitization of Lanthanide Luminescence by d-Block Metal-to-Ligand Charge-Transfer Excited States. *J. Am. Chem. Soc.* **2004**, *126*, 9490−9491.
(32) Sambrook, M. R.; Curiel, D.; Hayes, E. J.; Beer, P. D.; Pope, S. J. A.; Faulkner, S. Sensitised near infrared emission from lanthanides via anion-templated assembly of d-f heteronuclear [2]-pseudorotaxanes. *New J. Chem.* **2006**, *30*, 1133−1136.
(33) Ishida, H.; Tobita, S.; Hasegawa, Y.; Katoh, R.; Nozaki, K. Recent Advances in Instrumentation for Absolute Emission Quantum Yield Measurements. *Coord. Chem. Rev.* **2010**, *254*, 2449−2458.
(34) Frisch, M. J.; Trucks, G. W.; Schlegel, H. B.; Scuseria, G. E.; Robb, M. A.; Cheeseman, J. R.; Scalmani, G.; Barone, V.; Mennucci, B.; Petersson, G. A.; Nakatsuji, H.; Caricato, M.; Li, X.; Hratchian, H. P.; Izmaylov, A. F.; Bloino, J.; Zheng, G.; Sonnenberg, J. L.; Hada, M.; Ehara, M.; Toyota, K.; Fukuda, R.; Hasegawa, J.; Ishida, M.; Nakajima, T.; Honda, Y.; Kitao, O.; Nakai, H.; Vreven, T.; Montgomery, J. A., Jr; Peralta, J. E.; Ogliaro, F.; Bearpark, M.; Heyd, J. J.; Brothers, E.; Kudin, K. N.; Staroverov, V. N.; Keith, T.; Kobayashi, R.; Normand, J.; Raghavachari, K.; Rendell, A.; Burant, J. C.; Iyengar, S. S.; Tomasi, J.; Cossi, M.; Rega, N.; Millam, J. M.; Klene, M.; Knox, J. E.; Cross, J. B.; Bakken, V.; Adamo, C.; Jaramillo, J.; Gomperts, R.; Stratmann, R. E.; Yazyev, O.; Austin, A. J.; Cammi, R.; Pomelli, C.; Ochterski, J. W.; Martin, R. L.; Morokuma, K.; Zakrzewski, V. G.; Voth, G. A.; Salvador, P.; Dannenberg, J. J.; Dapprich, S.; Daniels, A. D.; Farkas, O.; Foresman, J. B.; Ortiz, J. V.; Cioslowski, J.; Fox, D. J. *Gaussian 09*. Revision C.01; Gaussian Inc.: Wallingford CT, 2010;.
(35) (a) Dunning, T. H., Jr; Hay, P. J.. In *Modern Theoretical Chemistry*; SchaeferIII, H. F., Ed.; Plenum: New York, 1977; Vol. *3*, pp 1−28. (b) Kuechle, W.; Dolg, M.; Stoll, H.; Preuss, H. Ab initio pseudopotentials for HG through RN. 1. Parameter sets and atomic calculations. *Mol. Phys.* **1991**, *74*, 1245−1263.
(36) Ditchfield, R.; Hehre, W. J.; Pople, J. A. Self-Consistent Molecular-Orbital Methods. IX. An Extended Gaussian-Type Basis for Molecular-Orbital Studies of Organic Molecules. *J. Chem. Phys.* **1971**, *54*, 724−728.
(37) O'Boyle, N. M.; Tenderholt, A. L.; Langner, K. M. cclib: a library for package-independent computational chemistry algorithms. *J. Comput. Chem.* **2008**, *29*, 839−845.
(38) Sheldrick, G. M. ShelXT-Integrated space-group and crystal-structure determination. *Acta Crystallogr.* **2015**, *71*, 3−8.
(39) Dolomanov, O. V.; Bourhis, L. J.; Gildea, R. J.; Howard, J. A. K.; Puschmann, H. Olex2: A complete structure solution, refinement and analysis program. *J. Appl. Crystallogr.* **2009**, *42*, 339−341.
(40) Sheldrick, G. M. Crystal structure refinement with ShelXL. *Acta Crystallogr.* **2015**, *71*, 3−8.
(41) (a) Charbonnière, L. J.; Weibel, N.; Ziessel, R. F. 5'-Substituted-6-Carboxylic-2,2'-Bipyridine Acid: A Pivotal Architecton for Building Preorganized Ligands. *J. Org. Chem.* **2002**, *67*, 3933−3936. (b) Forato, F.; Belhboub, A.; Monot, J.; Petit, M.; Benoit, R.; Sarou-Kanian, V.; Fayon, F.; Jacquemin, D.; Queffelec, C.; Bujoli, B. Phosphonate-Mediated Immobilization of Rhodium/Bipyridine Hydrogenation Catalysts. *Chem.—Eur. J.* **2018**, *24*, 2457−2465. (c) Telfer, S. G.; Bernardinelli, G.; Williams, A. F. Iron and Cobalt Complexes of 5,5′-Di(Methylene-N-Aminoacidyl)-2,2′-Bipyridyl Ligands: Ligand Design for Diastereoselectivity and Anion Binding. *Dalton Trans.* **2003**, 435−440.
(42) A crystal structure has been reported: Park, S.; Moon, S.-H.; Kim, T. H.; Park, K.-M. *Acta Crystallogr.* **2011**, *E67*, o2392.
(43) (a) Balzani, V.; Ceroni, P.; Credi, A.; Venturi, M. Ruthenium Tris(Bipyridine) Complexes: Interchange between Photons and Electrons in Molecular-Scale Devices and Machines. *Coord. Chem. Rev.* **2021**, *433*, 213758. (b) Juris, A.; Balzani, V.; Barigelletti, F.; Campagna, S.; Belser, P.; von Zelewsky, A. Ru(II) Polypyridine Complexes: Photophysics, Photochemistry, Eletrochemistry, and Chemiluminescence. *Coord. Chem. Rev.* **1988**, *84*, 85−277.
(44) Boselli, L.; Carraz, M.; Mazeres, S.; Paloque, L.; Gonzalez, G.; Benoit-Vical, F.; Valentin, A.; Hemmert, C.; Gornitzka, H. Synthesis, Structures, and Biological Studies of Heterobimetallic Au(I)−Ru(II) Complexes Involving N-Heterocyclic Carbene-Based Multidentate Ligands. *Organometallics* **2015**, *34*, 1046−1055.
(45) Sullivan, B. P.; Salmon, D. J.; Meyer, T. J. Mixed Phosphine 2,2'-Bipyridine Complexes of Ruthenium. *Inorg. Chem.* **1978**, *17*, 3334−3341.
(46) Dongare, P.; Myron, B. D. B.; Wang, L.; Thompson, D. W.; Meyer, T. J. $[Ru(bpy)_3]^{2+}$ revisited. Is it localized or delocalized? How does it decay? *Coord. Chem. Rev.* **2017**, *345*, 86−107.
(47) Ishida, H.; Tobita, S.; Hasegawa, Y.; Katoh, R.; Nozaki, K. Recent Advances in Instrumentation for Absolute Emission Quantum Yield Measurements. *Coord. Chem. Rev.* **2010**, *254*, 2449−2458.
(48) Sveshnikova, E. B.; Shakhverdov, P. A.; Shakhverdov, T. A.; Lanin, V. E.; Safina, R. U.; Bolotin, B. M.; Ermolaev, V. L. Luminescence of dipicolinic complexes of lanthanide ions. *Opt. Spectrosc.* **2003**, *95*, 898−907.

https://doi.org/10.1021/acs.inorgchem.3c02352
Inorg. Chem. 2023, 62, 19446−19456